Channel Gain Modeling Through an Intelligent Reflecting Surface

Jason K. Bingham, *Senior Member, IEEE*, Md Sadman Siraj, and Eirini Eleni Tsiropoulou, *Senior Member, IEEE*

***Abstract*—Recently, Intelligent Reflecting Surfaces (IRSs) with controllable substructures have attracted attention due to their ability to manipulate electromagnetic wave reflections. A key benefit of IRSs is their capacity to enhance signal gain at the receiver. In this article, we propose a general channel gain model suitable for various wireless communication setups. We start with the gain models for the basic Single-Input Single-Output (SISO) case, progressing to the general model in the Multiple-Input Multiple-Output (MIMO) scenario. The models simplify for specific parameter choices. Also, we determine the optimal phase of IRS atoms for maximizing gain.**

***Index Terms*—Intelligent Reflecting Surface, Reconfigurable Intelligent Surface, Channel Gain, Phase Optimization.**

I. INTRODUCTION

Electromagnetic waves propagate through an environment and reflect off encountered surfaces to create indirect signals at a receiver. The indirect signals range over a spectrum from purely specular to purely diffuse and result in destructive multipath signals at a receiver except in specific cases. The specific case in which an indirect signal results in constructive multipath is when a receiver is located where the phase of the indirect signal is matched with the direct signal.

Intelligent Reflecting Surfaces (IRSs), or alternatively Reconfigurable Intelligent Surfaces (RISs), are devices that control electromagnetic wave reflections to create a coherent signal at the receiver. Unlike uncontrolled reflections, which cause destructive interference, an IRS enables constructive interference, and enhances the signal strength or delivers signals to receivers obscured from the transmitter.

An IRS is typically constructed of sub-wavelength sized structures used to create a diverse impedance profile over the entire surface [1]. By intelligently changing the impedance of each structure, the phase and possibly magnitude of the electromagnetic field scattered by the structure may be changed. These changes allow the overall reflection to be focused toward a desired location and arrive with a controlled phase. The individual structures of an IRS are often referred to as elements [2] or metaatoms [1]. We use the term ‘atom’ to refer to the substructures of an IRS.

A key factor in the design and control of an IRS is the channel gain, which is impacted by the size of the IRS, geometry of the channel, and the atom states [2]. Using an IRS in conjunction with a direct signal increases the channel gain at the receiver. Increasing the gain increases the signal-to-noise ratio (SNR) and ultimately can decrease the interference. It also may allow for decreasing the required transmitter power, reduces errors, and increases the transmission capacity [1].

Jason Bingham is with the Department of Electrical and Computer Engineering, University of New Mexico, USA (email: jasonkbingham@unm.edu). Md Sadman Siraj, and Dr. Eirini Eleni Tsiropoulou are with the Performance and Resource Optimization in Networks – PROTON Lab, School of Electrical, Computer and Energy Engineering, Arizona State University, USA (email: {msiraj13, eirini}@asu.edu). The research of Dr. Tsiropoulou was partially supported by the NSF Awards #2219617 and #2319994.

A. Related Work

Holistic channel gain modeling has been tackled by many authors. Typically, the models are only as complex as needed for the intended application or only cover the necessary conditions to satisfy the environmental conditions and/or system design. Much of the remaining literature, such as [3], delve straight into developing system models without a need to develop the channel gain. To our knowledge, no single model has been developed to cover the numerous conditions under which channel gain modeling is needed. A simple model is derived in [4] based on the conventional two-way channel model for wireless communications. This model demonstrates the superiority of IRS use in wireless communications [5]. However, as also pointed out by [5], the model omits complexities such as the size and dimension of the atoms and the incident and reflected signal angles. In [2], the author develops a comprehensive model that builds from basic signal propagation and power transmission models. This model is an excellent starting basis for a Single-Input Single-Output (SISO) channel configuration. This model needs to be expanded to cover more complicated transmission configurations. A more detailed and thorough discussion of system models is provided in [1]. However, the focus of the book is more on channel capacity than on channel gain.

B. Contributions & Outline

In this article, we develop a general channel gain model applicable to most wireless communications setups. We discuss the over-the-air gain models applicable to all scenarios and then identify a basic IRS configuration. We start by developing the channel gain models for the simple SISO case and expand into the Multiple-Input Single-Output (MISO) and Single-Input Multiple-Output (SIMO) cases. Finally, we complete the general model using the Multiple-Input Multiple-Output (MIMO) case, which covers the earlier cases when parameters are chosen accordingly. Also, we provide the corresponding models for determining the optimal phase of the IRS atoms.

II. MAIN CONTRIBUTIONS

The IRS channel is the signal path from a transmitter to a receiver that passes through an IRS. Since the channel through an IRS is indirect, it is indicated using a subscript i and the direct channel is indicated using a subscript d. The channel is divided into three segments: 1) an over-the-air channel from the transmitter to the IRS (subscript t), 2) the tuneable reflection (subscript ψ), and 3) an over-the-air channel from the IRS to the receiver (subscript r). The IRS channel is shown by the solid red line in Fig. 1.

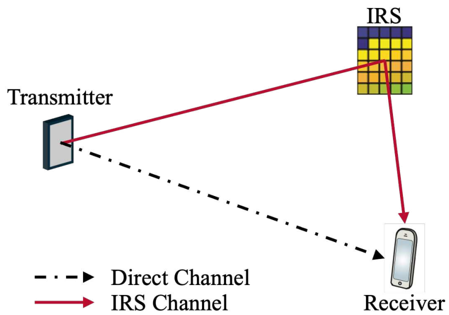

Fig. 1: IRS Channel

Note that the direct path from the transmitter to the receiver is not included in the definition of the channel but will be used later for the computation of the atoms' optimal phase shift.

A. Over-the-Air Path Gains

The over-the-air path gains from the transmitter to the IRS (β_t) and from the IRS to the receiver (β_r) can be modeled in many ways. The simplest and most common model (Eq. 1) is derived from the Friis transmission formula [6] where λ is the signal wavelength and d is the Euclidean distance between the signal origin and destination.

$$\beta = \left(\frac{\lambda}{4\pi d}\right)^2 \tag{1}$$

Other models like the non-line-of-sight (NLoS) urban microcell (UMi) scenario [7] can be used for path gain, but care is needed to avoid duplicating NLoS gains.

B. IRS

A common reference frame, an understanding of the IRS layout, and knowledge of the atom localization are needed to simplify the channel gain computations.

1) Reference Frame: The IRS reference frame (superscript i) is defined from the IRS's perspective, with the origin at its center. The x-axis points away from the IRS into the signal space, normal to the surface. The y-axis lies in the IRS plane, pointing to the right, while the z-axis points downward. This forms a right-handed, orthogonal coordinate system, as shown by the red arrows in Fig. 2, with the signal space located behind the page. This reference frame is applicable regardless of the IRS configuration.

2) Layout: The basic IRS layout is a rectangular array of atoms with M_h columns (horizontal) and M_v rows (vertical). The total number of atoms is therefore $M = M_h M_v$ and the individual atoms are numbered as $m \in 0 \dots M-1$. In later discussions, L will denote the number of transmit antennas, and N the number of receive antennas. Element numbering for l and n is the same as for m.

The spacing between the centers of any two adjacent atoms is Δ, which is a fraction of the wavelength. The width (Eq. 2) and height (Eq. 3) of the IRS are therefore dependent on the wavelength, the number of atoms, and the IRS layout.

$$w = \Delta M_h \tag{2}$$
$$h = \Delta M_v \tag{3}$$

If M_h or M_v are equal to 1, then the IRS is a vertical or horizontal uniform linear array (ULA) respectively. When both M_h and M_v are greater than 1, the IRS is a uniform planar array (UPA). An example IRS configuration with $M_h = 5$ and $M_v = 6$ is shown in Fig. 2.

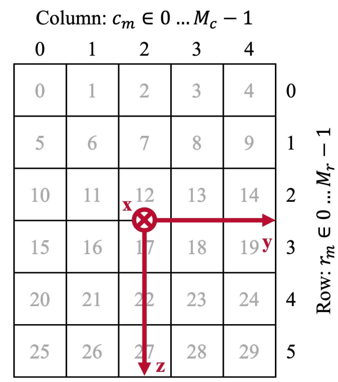

Fig. 2: IRS Layout

Other IRS configurations, e.g., hexagonal arrays, are possible, with atom localization equations left to the reader.

3) Atom Position: For the rectangular layout, the upper left atom of the IRS is designated as $m = 0$ and the lower right atom $m = M - 1$. The column (Eq. 4) and row (Eq. 5) of each atom m are functions of the atom number.

$$c(m) = m \bmod M_h \tag{4}$$
$$r(m) = \left\lfloor \frac{m}{M_h} \right\rfloor \tag{5}$$

The atom, column, and row numbers for the example layout are shown in Fig. 2.

Within the defined IRS reference frame, the positions (Eq. 6) of the atoms are computed from the column and row positions, and the IRS height and width. Each row of Eq. 6 is an atom and the columns are the x, y and z coordinates respectively.

$$\boldsymbol{P}_m^i = \begin{bmatrix} 0 & \Delta c(0) - w/2 & \Delta r(0) - h/2 \\ 0 & \Delta c(1) - w/2 & \Delta r(1) - h/2 \\ \vdots & \vdots & \vdots \\ 0 & \Delta c(m) - w/2 & \Delta r(m) - h/2 \\ \vdots & \vdots & \vdots \\ 0 & \Delta c(M-1) - w/2 & \Delta r(M-1) - h/2 \end{bmatrix} \tag{6}$$

C. SISO End-to-End Channel Configuration

In a SISO channel configuration, the signal leaves a single transmit antenna $(L = 1)$ located at $\boldsymbol{p}_t^i = [x_t^i, y_t^i, z_t^i]^T$ and experiences an over-the-air gain of β_{tm} on its way to an atom. The signal reflects off the atom, shifts phase, and experiences another over-the-air gain of β_{mr} on its way to the single receive antenna $(N = 1)$ at $\boldsymbol{p}_r^i = [x_r^i, y_r^i, z_r^i]^T$.

The signal arrives at and departs from the atom along the unit vectors $\hat{\boldsymbol{r}}_{mt}^i$ and $\hat{\boldsymbol{r}}_{mr}^i$ respectively. As the signal enters the atom it experiences a gain of $\beta_m(\hat{\boldsymbol{r}}^i_{mt})$ that is proportional to the effective area of the element as seen from the transmitter. Likewise, it experiences a gain of $\beta_m(\hat{\boldsymbol{r}}^i_{mr})$ that is proportional to the effective area of the element as seen from the receiver. Example unit vectors are shown in Fig. 3.

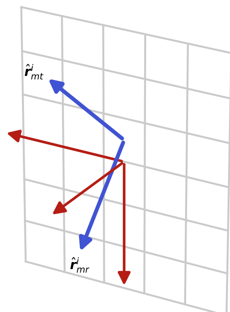

Fig. 3: Example Unit Vectors

1) Atom Response: The incident (Eq. 7) and reflected (Eq. 8) responses of each atom [1] are modeled using knowledge of the atom positions (Eq. 6) and the vectors of arrival and departure.

$$\mathrm{a}_{t,m} = e^{\mathrm{j}2\pi/\lambda\ \boldsymbol{P}^i_m \cdot \hat{\boldsymbol{r}}^i_{mt}} \quad (7) \qquad \mathrm{a}_{r,m} = e^{\mathrm{j}2\pi/\lambda\ \boldsymbol{P}^i_m \cdot \hat{\boldsymbol{r}}^i_{mr}} \quad (8)$$

2) Channel Coefficients: Using the path gains (Eq. 1) and atom responses $\mathbf{a}_t \in \mathbb{C}^{M\times 1}, \mathbf{a}_r \in \mathbb{C}^{1\times M}$, we model the transmit (Eq. 9) and receive segment (Eq. 10) atom coefficients using Rician fading. In the coefficients, $\kappa_d = \sqrt{\kappa/(\kappa+1)}$ and $\kappa_i = \sqrt{1/(\kappa+1)}$ describe the relationship of the direct (i.e., line-of-sight (LoS)) and indirect (i.e., NLoS) signals in the channel segment, and $\mathcal{Z}$ is a complex standard normal random value modeling the NLoS gain.

$$\mathrm{h}_{t,m} = \sqrt{\beta_{tm}\beta_m(\hat{\boldsymbol{r}}^i_{mt})}\,[\kappa_d\ \mathrm{a}_{t,m} + \kappa_i\ \mathcal{Z}] \quad (9)$$

$$\mathrm{h}_{r,m} = \sqrt{\beta_{mr}\beta_m(\hat{\boldsymbol{r}}^i_{mr})}\ \mathrm{a}_{r,m} \quad (10)$$

When $\kappa = 0$ $(\kappa_d = 0, \kappa_i = 1)$ the LoS signal is fully blocked and the destination only sees NLoS signals. With $\kappa = 1$ $(\kappa_d = 0.5, \kappa_i = 0.5)$ the strength of the LoS sub-channel is equal to the NLoS sub-channel. Finally, $\kappa = \infty$ $(\kappa_d = 1, \kappa_i = 0)$ is the pure LoS case. The receive segment does not use Rician fading as the IRS supplies a directional signal and there exists negligible NLoS signals at the receiver.

The atom subchannel coefficients (Eq. 9, 10) of all the atoms may be combined into full channel coefficients (Eq. 11, 12). If the IRS is in the far field of the transmitter and the receiver is in the far field of the IRS then the over-the-air path gains $\boldsymbol{\beta}_{ti}$ and $\boldsymbol{\beta}_{ir}$ may be reduced to scalars.

$$\mathbf{h}_t = \sqrt{\boldsymbol{\beta}_{ti}\boldsymbol{\beta}_m(\hat{\boldsymbol{r}}^i_{mt})}\,[\kappa_d\ \mathbf{a}_t + \kappa_i\ \mathcal{Z}] \qquad \in \mathbb{C}^{M\times 1} \quad (11)$$

$$\mathbf{h}_r = \sqrt{\boldsymbol{\beta}_{ir}\boldsymbol{\beta}_m(\hat{\boldsymbol{r}}^i_{mr})}\ \mathbf{a}_r \qquad \in \mathbb{C}^{1\times M} \quad (12)$$

3) Channel Model and Gain: Combining the two subchannel coefficients (Eq. 9, 10) with the controllable atom phase shift (ψ_m) provides the end-to-end subchannel model (Eq. 13) for an atom.

$$\mathrm{h}_m = \mathrm{h}_{r,m} e^{j\psi_m} \mathrm{h}_{t,m} \quad (13)$$

The subchannels are summed to get the end-to-end IRS channel model (Eq. 14) and then the magnitude of the channel model is squared to get the channel gain (Eq. 15).

$$\mathrm{h}_i = \sum_{m=0}^{M-1} \mathrm{h}_m = \sum_{m=0}^{M-1} \mathrm{h}_{r,m} e^{j\psi_m} \mathrm{h}_{t,m} \quad (14)$$

$$\beta = |\mathrm{h}_I|^2 = \left| \sum_{m=0}^{M-1} \mathrm{h}_{r,m} e^{j\psi_m} \mathrm{h}_{t,m} \right|^2 \quad (15)$$

The array form of the channel model (Eq. 16) provides for quicker computations where $\mathbf{D}_\psi$ is the diagonal matrix of controlled phase shifts (Eq. 17). This then gives the array form of the full channel path gain (Eq. 18).

$$\mathrm{h} = \mathbf{h}_r \mathbf{D}_\psi \mathbf{h}_t \qquad \in \mathbb{C}^{1\times 1} \quad (16)$$

$$\mathbf{D}_\psi = \mathrm{diag}\left(e^{j\psi_0}, \ldots, e^{j\psi_{M-1}}\right) \qquad \in \mathbb{C}^{M\times M} \quad (17)$$

$$\beta = |\mathbf{h}_r \mathbf{D}_\psi \mathbf{h}_t|^2 \quad (18)$$

4) Phase Optimization: To maximize the channel path gain, the signal phase in each atom's subchannel must align with those in all other subchannels. Thus, the phase (ψ) of atom m (Eq. 19) is set to the difference of a desired phase at the receiver's antenna (ψ_r) and the phase of the subchannel at the receiver with zero phase shift $(\arg(\mathrm{h}_{r,m}\mathrm{h}_{m,t}))$. The phase is adjusted with an integer k_m to assure that $\psi_m \in [-\pi, \pi)$ [1].

$$\psi_m = \psi_r - \arg(\mathrm{h}_{r,m}\mathrm{h}_{m,t}) + 2\pi k_m \quad (19)$$

To calculate all phases simultaneously, Eq. 19 for all atoms is combined into the array form (Eq. 20).

$$\boldsymbol{\psi} = \psi_r - \arg(\mathbf{h}_r^T \mathbf{h}_t) + 2\pi \boldsymbol{k} \qquad \in \mathbb{C}^{M\times 1} \quad (20)$$

One possible solution of the phase optimization [1] is to align the phases of all signals to the phase of the signal that would come directly from the transmitter (Eq. 21).

$$\psi_r = \arg(\mathrm{h}_d) \quad (21)$$

D. MISO End-to-End Channel Configuration

In a MISO channel configuration, the transmitter is a multi-element antenna array $(L > 1)$ and the receiver is a single antenna $(N = 1)$. Therefore, Eq. 9 requires an update to include the departure response of the transmitter elements (Eq. 22). The departure response is computed using the position of the transmitter elements $(\boldsymbol{P}^t_l)$ and the departure vector to the IRS $(\hat{\boldsymbol{r}}^t_{li})$. The positions and vector are calculated in the same manner as they are for the atoms but using a transmitter reference frame (superscript t).

$$\mathrm{t}_{i,l} = e^{\mathrm{j}2\pi/\lambda\ \boldsymbol{P}^t_l \cdot \hat{\boldsymbol{r}}^t_{li}} \qquad \in \mathbb{C}^{1\times L} \quad (22)$$

1) Channel Coefficients: The new transmit segment channel coefficient (Eq. 23) incorporates the response of the transmitter elements (Eq. 22) using Rician fading.

$$\mathrm{h}_{t,lm} = \sqrt{\beta_{lm}\beta_m(\hat{\boldsymbol{r}}^i_{mt})}\,[\kappa_d\ \mathrm{a}_{t,m}\ \mathrm{t}_{i,l} + \kappa_i\ \mathcal{Z}] \quad (23)$$

However, as the transmitter supplies a directional signal, there are minimal NLoS subchannels and as $\kappa \to \infty$ then $\kappa_d \to 1$

and $\kappa_i \to 0$, providing a reduced channel coefficient (Eq. 24).

$$\mathrm{h}_{t,lm} = \sqrt{\beta_{t,lm}\beta_m(\hat{\boldsymbol{r}}^i_{mt})}\ \mathrm{a}_{t,m}\ \mathrm{t}_{i,l} \quad (24)$$

When combining Eq. 24 for all atoms, an $M \times L$ matrix (Eq. 25) results instead of the $M \times 1$ array in Eq. 11 due to the added transmitter element responses.

$$\mathbf{H}_t = \sqrt{\boldsymbol{\beta}_{ti}\boldsymbol{\beta}_m(\hat{\boldsymbol{r}}^i_{mt})}\ \mathbf{a}_t\mathbf{t}_i \quad \in \mathbb{C}^{M\times L} \quad (25)$$

The receive segment channel coefficient remains the same as in the SISO configuration.

2) Channel Model and Gain: To create the end-to-end MISO channel model (Eq. 26) and gain (Eq. 27) perform two summations. One over all of the transmitter element responses and another over all of the atom responses.

$$\mathrm{h} = \sum_{m=0}^{M-1}\sum_{l=0}^{L-1} \mathrm{h}_{r,m} e^{j\psi_m} \mathrm{h}_{t,lm} \quad (26)$$

$$\beta = \left| \sum_{m=0}^{M-1}\sum_{l=0}^{L-1} \mathrm{h}_{r,m} e^{j\psi_m} \mathrm{h}_{t,lm} \right|^2 \quad (27)$$

The array form of the channel model (Eq. 26) results in an array (Eq. 28) instead of a scalar, and the full channel gain of a MISO channel through an IRS is modeled as (Eq. 29).

$$\mathbf{h} = \mathbf{h}_r\mathbf{D}_\psi\mathbf{H}_t \in \mathbb{C}^{1\times L} \quad (28) \qquad \beta = |\mathbf{h}_r\mathbf{D}_\psi\mathbf{H}_t|^2 \quad (29)$$

3) Phase Optimization: Phase optimization of the atoms may be performed by either of two methods. First, extract the channel coefficients of one transmitter element from $\mathbf{H}_t$ (i.e., one column) to get $\mathbf{h}_t$ and then use (Eq. 20) to compute the phases. Or second, as the transmitter would be set up to provide L signals that are in phase at the IRS, sum $\mathbf{H}_t$ across all of the transmitter elements (Eq. 30). In the array form (Eq. 31) the summation is performed by $\mathbf{H}_t\mathbf{1}_L$ where $\mathbf{1}_L$ is a vertical array of L ones.

$$\psi_m = \psi_r - \arg\left(\mathrm{h}_{r,m}\left[\sum_{l=0}^{L-1}\mathrm{h}_{t,lm}\right]\right) + 2\pi k_m \quad (30)$$

$$\boldsymbol{\psi} = \psi_r - \arg\left(\mathbf{h}_r^T\left[\mathbf{H}_t\mathbf{1}_L\right]\right) + 2\pi\boldsymbol{k} \quad \in \mathbb{C}^{M\times 1} \quad (31)$$

E. SIMO End-to-End Channel Configuration

In SIMO, the transmitter uses a single antenna ($L = 1$), and the receiver employs a multi-element antenna array ($N > 1$). Thus, Eq. 10 needs to be updated to include the receiver elements' arrival response (Eq. 32), computed from the receiver element positions ($\boldsymbol{P}^r_n$) and the arrival vector from the IRS ($\hat{\boldsymbol{r}}^r_i$), both calculated similarly to the atom positions but in the receiver reference frame (superscript r).

$$\mathrm{r}_{i,n} = e^{\mathrm{j}2\pi/\lambda\ \boldsymbol{P}^r_n\cdot\hat{\boldsymbol{r}}^r_i} \quad \in \mathbb{C}^{N\times 1} \quad (32)$$

1) Channel Coefficients: The new receive segment channel coefficient (Eq. 33) incorporates the response of the receiver elements (Eq. 32).

$$\mathrm{h}_{r,mn} = \sqrt{\beta_{mn}\beta_m(\hat{\boldsymbol{r}}^i_{mr})}\ \mathrm{r}_{i,n}\ \mathrm{a}_{r,m} \quad (33)$$

When combining Eq. 33 for all atoms, an $N \times M$ matrix (Eq. 34) is produced instead of the $1 \times M$ array result of Eq. 12. This is due to adding the receiver element responses.

$$\mathbf{H}_r = \sqrt{\boldsymbol{\beta}_r\boldsymbol{\beta}_m(\hat{\boldsymbol{r}}^i_{mr})}\ \mathbf{r}_i\mathbf{a}_r \quad \in \mathbb{C}^{N\times M} \quad (34)$$

The transmit segment channel coefficient remains the same as in the SISO configuration.

2) Channel Model and Gain: To create the end-to-end MISO channel model (Eq. 35) and gain (Eq. 36), perform two summations: one over the atom responses and another over the receiver element responses.

$$\mathrm{h} = \sum_{n=0}^{N-1}\sum_{m=0}^{M-1} \mathrm{h}_{r,mn} e^{j\psi_m} \mathrm{h}_{t,m} \quad (35)$$

$$\beta = \left| \sum_{n=0}^{N-1}\sum_{m=0}^{M-1} \mathrm{h}_{r,mn} e^{j\psi_m} \mathrm{h}_{t,m} \right|^2 \quad (36)$$

The array form of the channel model (Eq. 35) leads to an array (Eq. 37) instead of a scalar, with the full channel gain of a SIMO channel through an IRS modeled as Eq. 38.

$$\mathbf{h} = \mathbf{H}_r\mathbf{D}_\psi\mathbf{h}_t \in \mathbb{C}^{N\times 1} \quad (37) \qquad \beta = |\mathbf{H}_r\mathbf{D}_\psi\mathbf{h}_t|^2 \quad (38)$$

3) Phase Optimization: Once again there exist two methods for performing the phase optimization. The channel coefficients of one receiver element from $\mathbf{H}_r$ (i.e., one row) may be extracted to get $\mathbf{h}_r$ and then use Eq. 20 to compute the phases, or $\mathbf{H}_r$ may be summed across all of the receiver elements (Eq. 39). In the array form (Eq. 40) the summation is performed by $\mathbf{H}_r^T\mathbf{1}_N$ where $\mathbf{1}_N$ is a vertical array of N ones.

$$\psi_m = \psi_r - \arg\left(\left[\sum_{n=0}^{N-1}\mathrm{h}_{r,mn}\right]\mathrm{h}_{t,m}\right) + 2\pi k_m \quad (39)$$

$$\boldsymbol{\psi} = \psi_r - \arg\left(\left[\mathbf{H}_r^T\mathbf{1}_N\right]\mathbf{h}_t\right) + 2\pi\boldsymbol{k} \quad \in \mathbb{C}^{M\times 1} \quad (40)$$

F. MIMO End-to-End Channel Configuration

The MIMO configuration of an IRS channel is the general configuration. In this configuration, both the transmitter and receiver are multi-element antenna arrays. The configuration uses both the transmit segment coefficient from II-D1 and the receive segment coefficient from II-E1.

1) Channel Model and Gain: The end-to-end MIMO channel model (Eq. 41) and gain (Eq. 42) requires three summations. One over all of the transmitter element responses, a second over all of the atom responses, and the final over all of the receiver element responses.

$$\mathrm{h} = \sum_{n=0}^{N-1}\sum_{m=0}^{M-1}\sum_{l=0}^{L-1} \mathrm{h}_{r,mn} e^{j\psi_m} \mathrm{h}_{t,lm} \quad (41)$$

$$\beta = \left| \sum_{n=0}^{N-1}\sum_{m=0}^{M-1}\sum_{l=0}^{L-1} \mathrm{h}_{r,mn} e^{j\psi_m} \mathrm{h}_{t,lm} \right|^2 \quad (42)$$

The array forms of the full channel model (Eq. 43) and gain (Eq. 44) of a MIMO channel through an IRS utilize the

This article has been accepted for publication in IEEE Networking Letters. This is the author's version which has not been fully edited and content may change prior to final publication. Citation information: DOI 10.1109/LNET.2025.3575096

channel coefficients (Eq. 25) and (Eq. 34).

$$\mathbf{H} = \mathbf{H}_r \mathbf{D}_\psi \mathbf{H}_t \quad \in \mathbb{C}^{N \times L} \tag{43}$$

$$\beta = \left|\mathbf{H}_r \mathbf{D}_\psi \mathbf{H}_t\right|^2 \tag{44}$$

2) Phase Optimization: For the MIMO configuration there are four possible procedures for calculating the optimal atom phases. The first three entail applying the techniques discussed in Sections II-C4, II-D3, or II-E3 and the fourth involves summing both $\mathbf{H}_t$ $\mathbf{H}_r$ across all of the relative elements (Eq. 45). Both the single atom (Eq. 45) and array form (Eq. 46) of the phase optimization combine the equations discussed in Sections II-D3 and II-E3.

$$\psi_m = \psi_r - \arg\left(\left[\sum_{n=0}^{N-1} \mathrm{h}_{r,mn}\right]\left[\sum_{l=0}^{L-1} \mathrm{h}_{t,lm}\right]\right) + 2\pi k_m \tag{45}$$

$$\boldsymbol{\psi} = \psi_r - \arg\left(\left[\mathbf{H}_r^T \mathbf{1}_N\right]\left[\mathbf{H}_t \mathbf{1}_L\right]\right) + 2\pi \boldsymbol{k} \quad \in \mathbb{C}^{M \times 1} \tag{46}$$

III. Numerical Results

We used the MIMO end-to-end channel configuration equations (Section II-F) to perform channel gain calculations in Python. The system model was configured with a 6×6 IRS, a single transmitter $100.499\,\mathrm{m}$ from the IRS along the vector $\hat{\mathbf{r}}_t^i = [0.995, 0.0, -0.0995]^T$, and a single receiver $72.961\,\mathrm{m}$ from the IRS along the vector $\hat{\mathbf{r}}_r^i = [0.984, 0.145, 0.1048]^T$. The initial phase of all IRS atoms were set to 0° and the SISO channel gain was computed with these settings. The atom phases were then optimized (Eq. 46) and the channel gain recomputed. We repeated the calculations increasing the IRS rows and columns until we reached a 200×200 UPA. The results are shown by the gray (0°) and red (optimal) lines in Fig. 4. The results are normalized so that $0\,\mathrm{dB}$ is equivalent to the free-space gain over $173.459\,\mathrm{m}$ $(t \to i \to r)$.

Optimization of the IRS atom phases increases the signal gain at the receiver by 3 to $38\,\mathrm{dB}$ depending on the IRS aperture and removes nulls evident in the zero phase results.

As the SISO calculations were processed, we also computed the gain of each configuration per [2] to verify our approach against published works. The Ellingson results are shown by the dashed yellow line in Fig. 4. The optimized SISO results differ from the Ellingson results by less than $0.000\,17\,\mathrm{dB}$ over the full range of IRS apertures. Mathematically, our model is the same as Ellingson's Eq. 11 when configured for SISO operation with free-space over-the-air gain.

Finally, we repeated the calculations using a 5×5 transmitter and receiver. The MIMO results are shown by the blue line in Fig. 4 and are an improvement over the optimized SISO configuration by $27.9\,\mathrm{dB}$ on average.

The results shown in Fig. 4 demonstrate the ability of an IRS of sufficient size to surpass free-space gains.

The results demonstrate the efficacy of our model, quantifying significant gains in the channel performance with phase optimization, particularly as the number of IRS elements increases. Our results align with [2], [5], which highlights the potential of IRSs to enhance signal gain, though this paper extends those insights by offering a more versatile and scalable model. Finally, the computational complexity of the proposed channel modeling, while scaling with the number of IRS atoms and antennas, is manageable with modern parallel hardware and offline optimization, which are practical for real-world deployment.

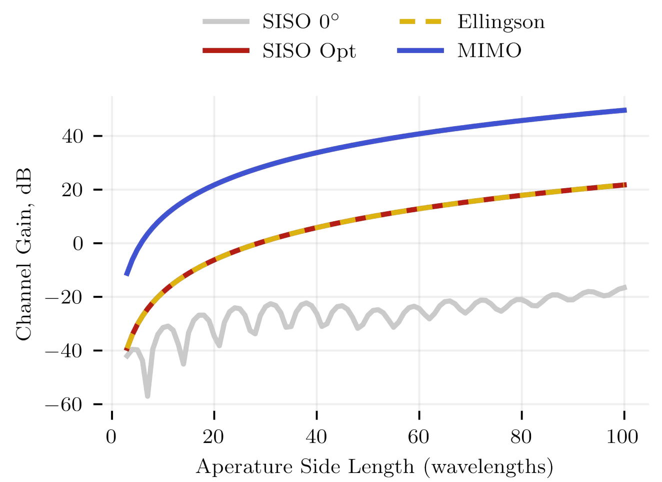

Fig. 4: Simulation Results

IV. Conclusions

A major advantage of an Intelligent Reflecting Surface is the ability to increase the signal gain at a receiver. In this article, we have presented a general model for the determination of the channel gain through an IRS that is applicable in most situations. We built the model up from the simplest case and finished with a complete model that may be configured for any channel and/or IRS configuration combination. At the same time we presented models for the optimization of the IRS atoms so that the channel gain can be maximized expediently. Finally, we presented the simulation results using the general model to demonstrate the potency of the channel gain equations. Part of our current and future work is the testing of the proposed model for practical hardware limitations like phase noise or mutual coupling, where these factors could impact the real-world performance by degrading phase precision and altering element responses.

References

[1] E. Björnson and Ö. T. Demir, *Introduction to Multiple Antenna Communications and Reconfigurable Surfaces*. Now Publishers, Inc., 2024.

[2] S. W. Ellingson, "Path loss in reconfigurable intelligent surface-enabled channels," in *IEEE 32nd Annual International Symposium on Personal, Indoor and Mobile Radio Communications*, 2021, pp. 829–835.

[3] Q. Wu, S. Zhang, B. Zheng, C. You, and R. Zhang, "Intelligent reflecting surface-aided wireless communications: A tutorial," *IEEE transactions on communications*, vol. 69, no. 5, pp. 3313–3351, 2021.

[4] E. Basar, M. Di Renzo, J. De Rosny, M. Debbah, M.-S. Alouini, and R. Zhang, "Wireless communications through reconfigurable intelligent surfaces," *IEEE access*, vol. 7, pp. 116 753–116 773, 2019.

[5] S. Gong, X. Lu, D. T. Hoang, D. Niyato, L. Shu, D. I. Kim, and Y.-C. Liang, "Toward smart wireless communications via intelligent reflecting surfaces: A contemporary survey," *IEEE Communications Surveys & Tutorials*, vol. 22, no. 4, pp. 2283–2314, 2020.

[6] H. T. Friis, "A Note on a Simple Transmission Formula," *Proceedings of the IRE*, vol. 34, no. 5, pp. 254–256, 1946.

[7] 3GPP, "Further advancements for E-UTRA physical layer aspects (Release 9)," 3GPP, Tech. Rep. 36.814, 2017.